

# 3D Volume Mesh Generation of Human Organs Using Surface Geometries Created from the Visible Human Data Set

John M. Sullivan, Jr., Ziji Wu, and Anand Kulkarni  
Worcester Polytechnic Institute  
Worcester, MA

[sullivan@wpi.edu](mailto:sullivan@wpi.edu)

## ABSTRACT:

Most medical imaging techniques produce two-dimensional image slices. These images are critical for diagnostic evaluations. However, they are rarely suitable for direct numerical analyses to solve bioengineering related problems involving electro-magnetic, thermal, or elastic situations. Our objective is to create valid numerical volume models of the anatomical geometries that are suitable for complete three-dimensional finite element solvers. These numerical models can provide the physician with quantitative data that might increase the probability of successful therapeutic treatments. This paper delineates the steps used to create three-dimensional volumetric meshes based on sequential two-dimensional images. The image dataset was taken directly from the Visible Human Project (VHP) dataset.

**KEYWORDS:** volume mesh generation, marching cube surface generation

## INTRODUCTION:

Advanced medical techniques frequently require geometric representations, rather than 2D photographic images, of human organs. These geometric models, either simulated or physical, can be used for analyses of physical problems, as well as visualization of organs for diagnosis, education, guided surgery, and other purposes. The Visible Human Project (VHP) has provided the input images and driving force necessary to develop strategies and techniques to create numerically consistent, quantitative data representations of anatomical geometries.

To create a volume mesh of organs from the medical images, one segments a set of medical images, such as cryosection images, MRI, or CT images. Surface boundary meshes are created from these segmented outlines for organs of interest. Finally solid volume meshes are created bounded by the surface meshes generated earlier. The flow chart for this procedure is shown in [Figure 1](#). The details of each step are discussed in the following sections.

A femur model created from VHP dataset illustrates the steps of the procedure for the sake of clarity. A multi-material volume mesh of the kidney region was used as the final example to show the capability of our system. The anatomical image slices of the Visible Male were used to create segmented outlines of the geometries. Slices 1851-2343 were located in the femur region and slices 1560-1690 were located within the kidney region.[\[1\]](#)

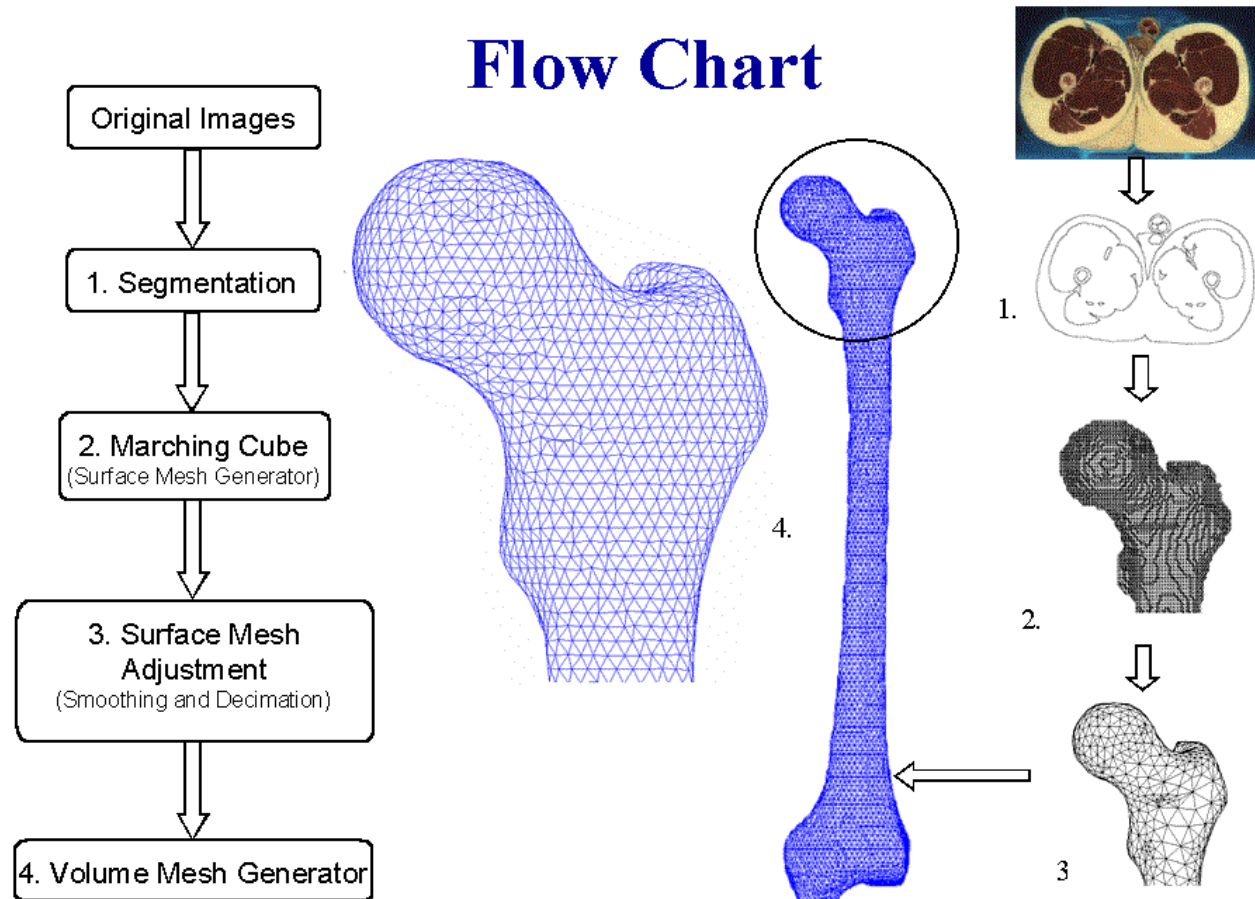


Figure 1. Flow Chart for Creation of Solid Volume Meshes Based on 2D Medical Images

### SEGMENTATION:

Medical images contain a significant amount of information besides the region of interests (ROIs), or more explicitly, the boundaries delineating these regions. In order to create three dimensional surfaces and volume meshes of ROIs we need to segment the original images, i.e., to outline each region of interest such that the enclosed area of the image can be flooded with a unique intensity value.

Automated segmentation of color images, as shown in [Figure 2](#), is still in its infancy. Consequently, we segmented the regions manually to represent boundaries of different materials. A unique pair of material IDs was assigned to each contour as in [Figure 3](#). A computationally efficient line-crossing algorithm was employed to classify each pixel within the image based on the segmented outline information only. [Figure 4](#) shows a segmented image. For kidney area, the 7.5 MB histological data files were reduced to 20 KB of segmented outline information.

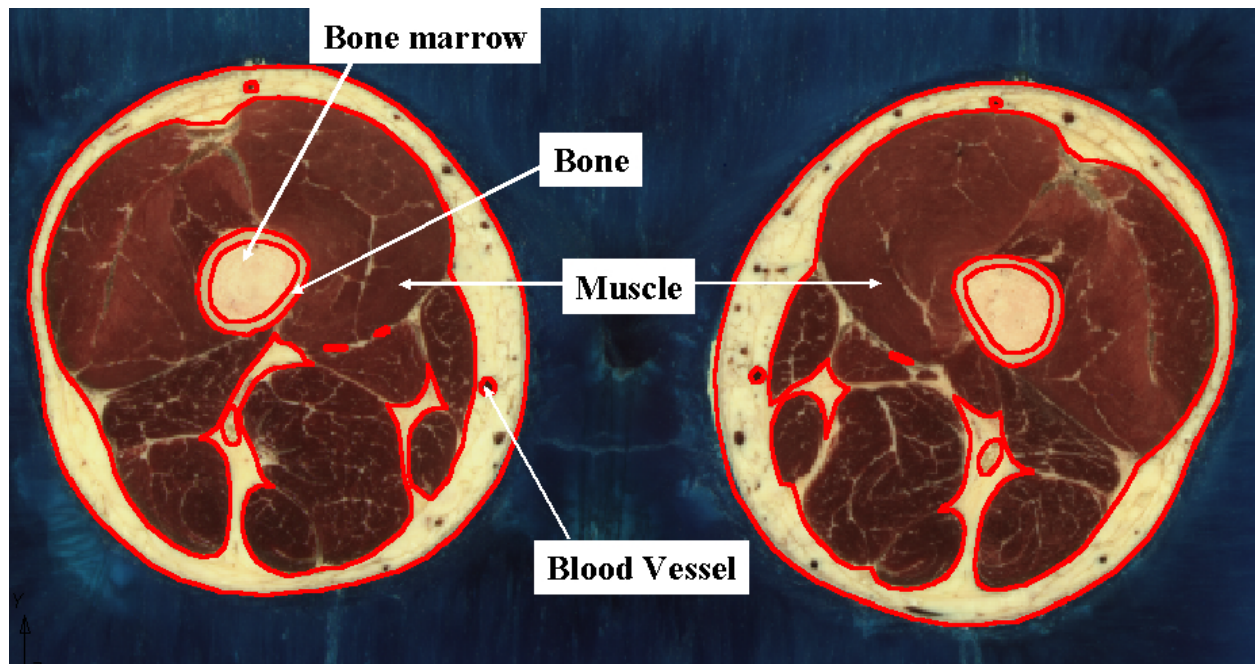


Figure 2. Manual Segmentation of Color Cryosections from the Visible Male

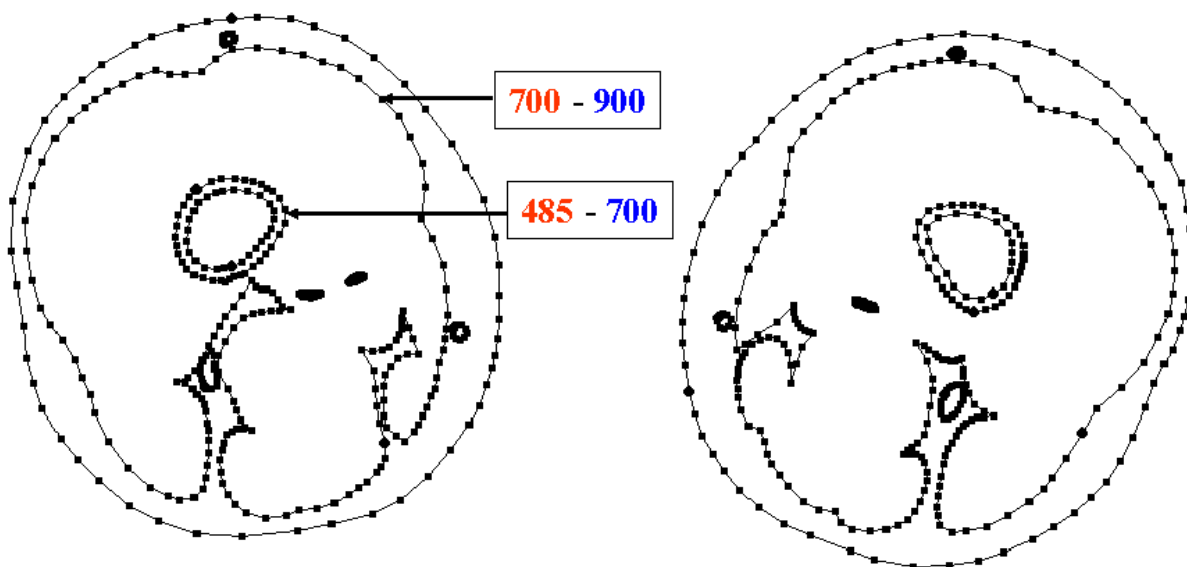


Figure 3. Each Boundary Line Segment is Assigned Two Material IDs Corresponding to Its Two Adjacent Materials, Ex: Fat=900, Muscle=700, Femur Bone=485

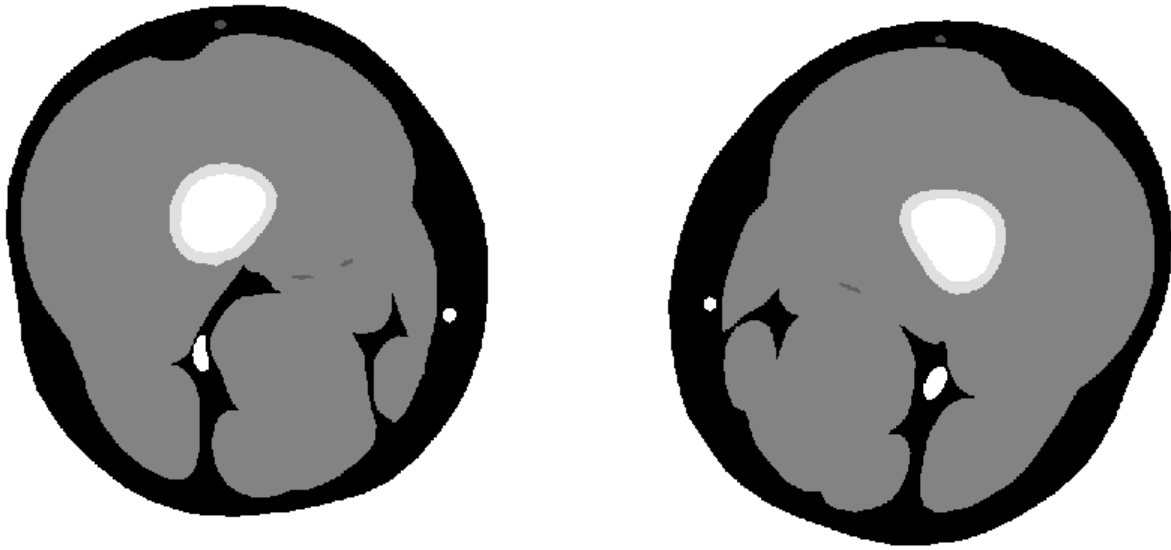


Figure 4. Segmented Image of the Original Cryosection Presented in [Figure 2](#)

#### **SURFACE MESH GENERATION:**

After creating segmented images, surface models were generated by utilizing a Marching Cube algorithm. A virtual cube, as in [Figure 5](#), was used to march through pairs of adjacent segmented images in a set.[\[2-4\]](#) The material information of cube's vertices was obtained directly from the two segmented images. If a vertex has a different material ID from its neighboring vertices, a boundary surface should exist between it and the others in order to separate different materials. There are 256 different combinations of material IDs that a cube's vertices could have. These combinations can be reduced to 15 situations with the use of symmetry. The surface generation process was extremely fast due to the direct triangulation from the look-up-table properties of the marching cube routine.[\[4\]](#)

As shown in [Figure 6](#), the surface model created by the Marching Cube algorithm has stair-step shaped surfaces, which do not represent the natural surface curvature. The model also contains too many nodes and triangle surfaces, which severely hinder the computational efficiency if used directly for volume mesh generation.

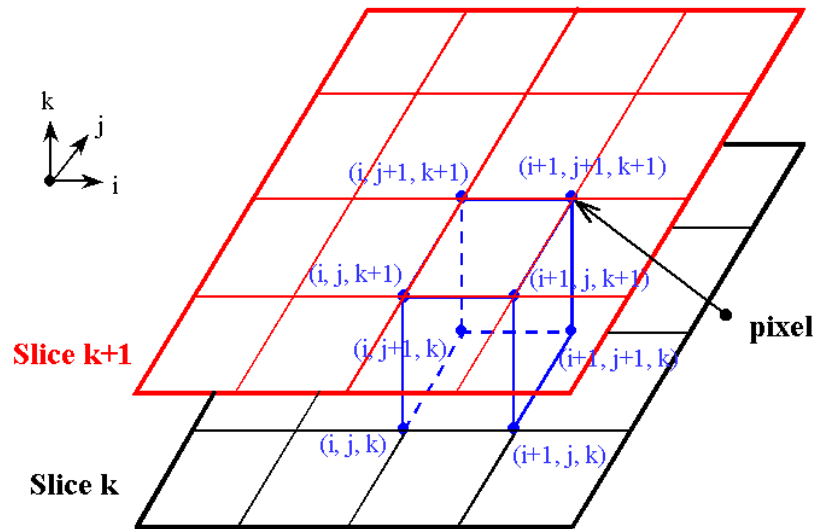


Figure 5. Illustration of Marching Cube Algorithm

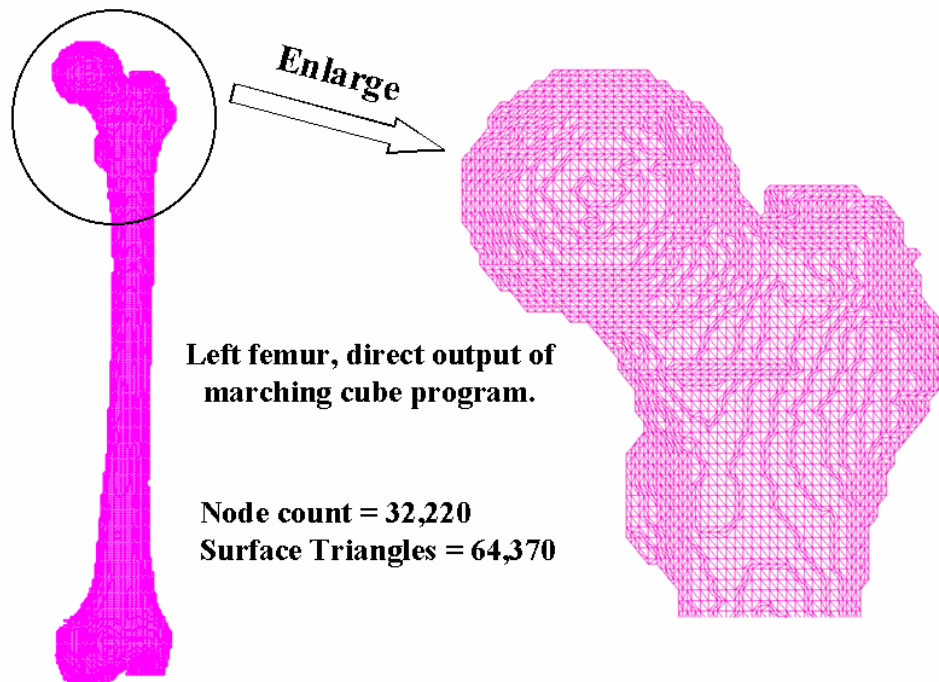


Figure 6. Surface Mesh of Femur Created from Segmented Images

## SURFACE MESH ADJUSTMENTS:

Generally speaking, there are two main procedures to improve the quality and efficiency of the existing surface model — smoothing and decimation.

Smoothing is a technique that adjusts the node coordinates to improve the appearance of a mesh, and/or improve the shape of surface triangles. During smoothing the topology of the model is not modified, only the geometry. A common and effective technique is Laplacian smoothing.<sup>[5]</sup> The Laplacian smoothing equation for a point  $p_i$  at position  $\vec{x}_i$  is given by

$$\vec{x}_{i+1} = \vec{x}_i + \lambda \sum (\vec{x}_j - \vec{x}_i) \quad \forall j: 0 \leq j < n$$

where  $\vec{x}_{i+1}$  is the new coordinate position, and  $\vec{x}_j$  are the positions of points  $p_j$  connected to  $p_i$ , and  $\lambda$  is a user-specified weight. [Figure 7](#) displays the surface model created from [Figure 6](#) after smoothing.

Contrary to the smoothing procedure, which does not change the number of nodes and triangles of a surface model, a decimation algorithm reduces the total number of surface triangles, while maintaining a good approximation to the original geometry. A smoothed and decimated surface model of femur is shown in [Figure 8](#). It only uses about 8% number of nodes and triangles to represent the geometry shown in previous figures.

Some of the surface triangles in [Figure 8](#) are relatively poor in quality. Though it is not a problem for our volume mesh generator, it could be a deficit for some other mesh generators. We applied a post-decimation smoothing step to improve the surface quality. The final resultant surface mesh, which serves as the input to the volume mesh generator, is shown in [Figure 9](#).

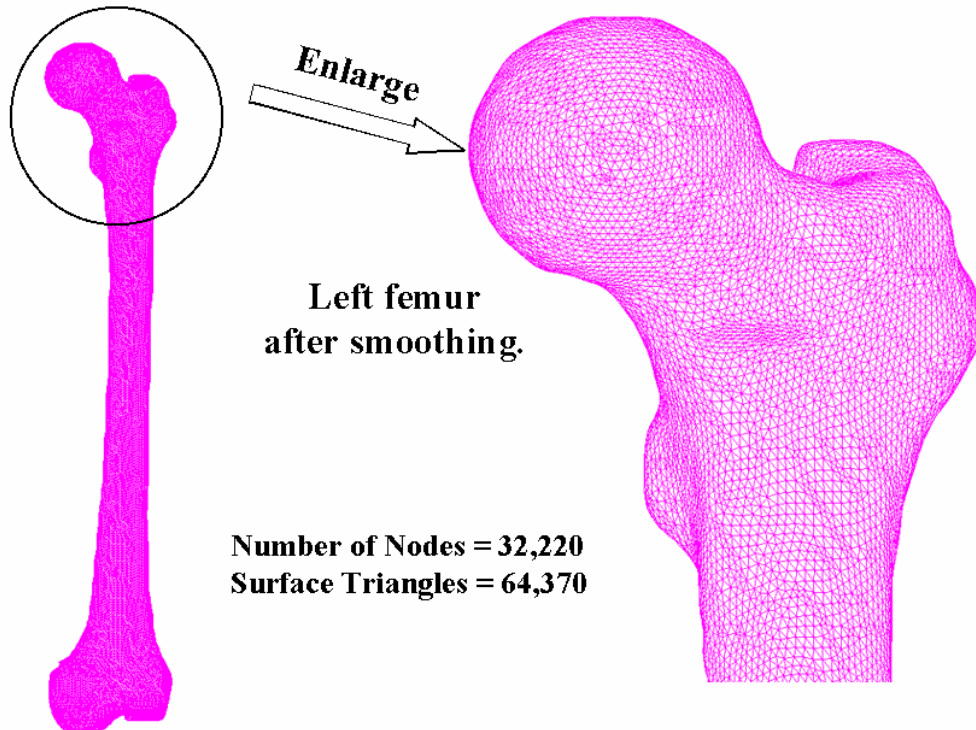


Figure 7. Smoothed Femur Surface Mesh



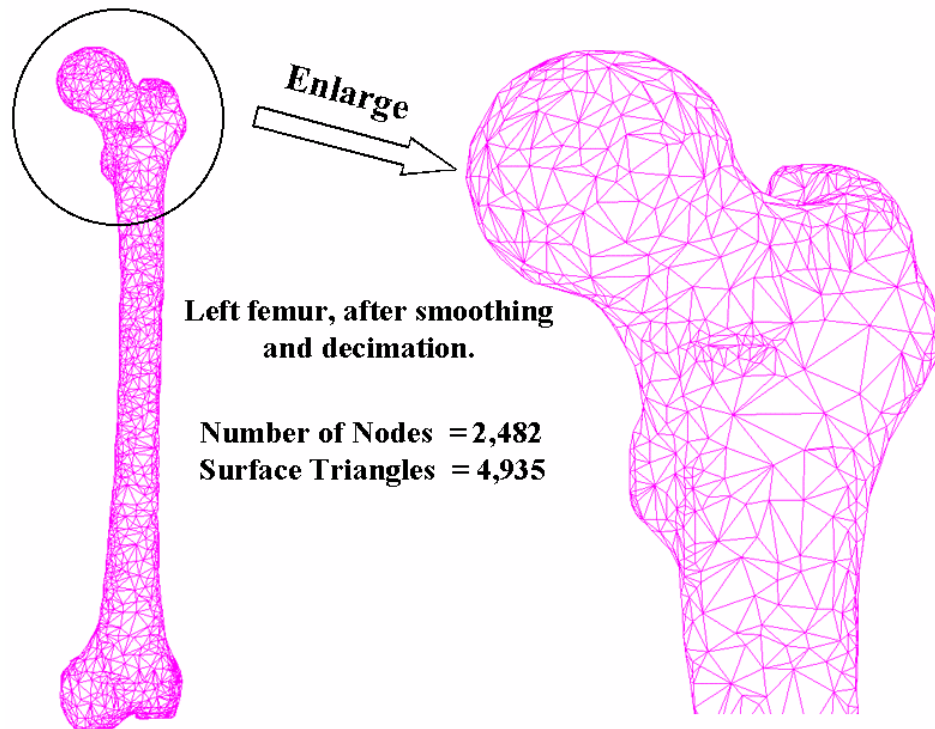


Figure 8. Smoothed and Decimated Femur Surface Mesh

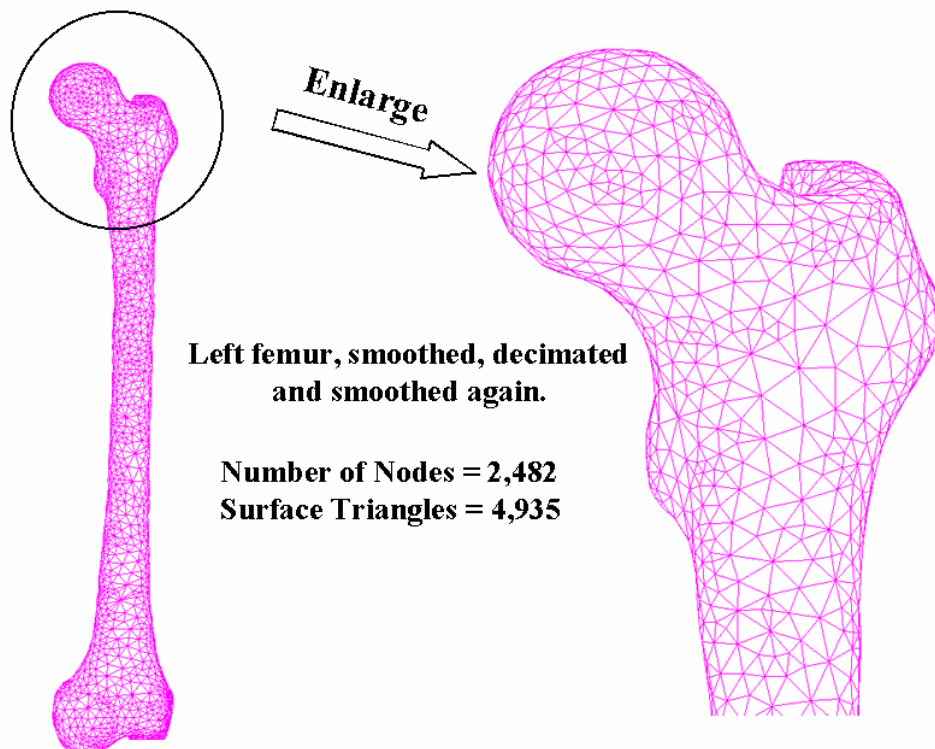


Figure 9. Final Femur Surface Mesh

## VOLUME MESH GENERATION:

Our three-dimensional, finite-element mesh generator [6-8] is a grid-based volume mesh generator, which is capable of describing arbitrary complex geometries exhibiting concave, convex, and planar surfaces.

A major feature in this work is the use of a deltahedral building block for the mesh generation. This building block unit creates a higher percentage of regular shaped tetrahedron mesh elements compared to existing strategies. A second critical feature of this mesh generation system is the ability to refine locally N levels without reducing the overall mesh quality. During the mesh generation process, all internal boundaries are preserved. In this mode material specific attributes can be assigned to each organ or tissue type. Consequently, finite element solutions of electro-magnetic wave propagation or other physics can be simulated on realistic full-body models.

As an example, the surface model in [Figure 9](#) was filled with 20,689 nodes and 102,742 tetrahedral volume elements as displayed in [Figure 10](#).

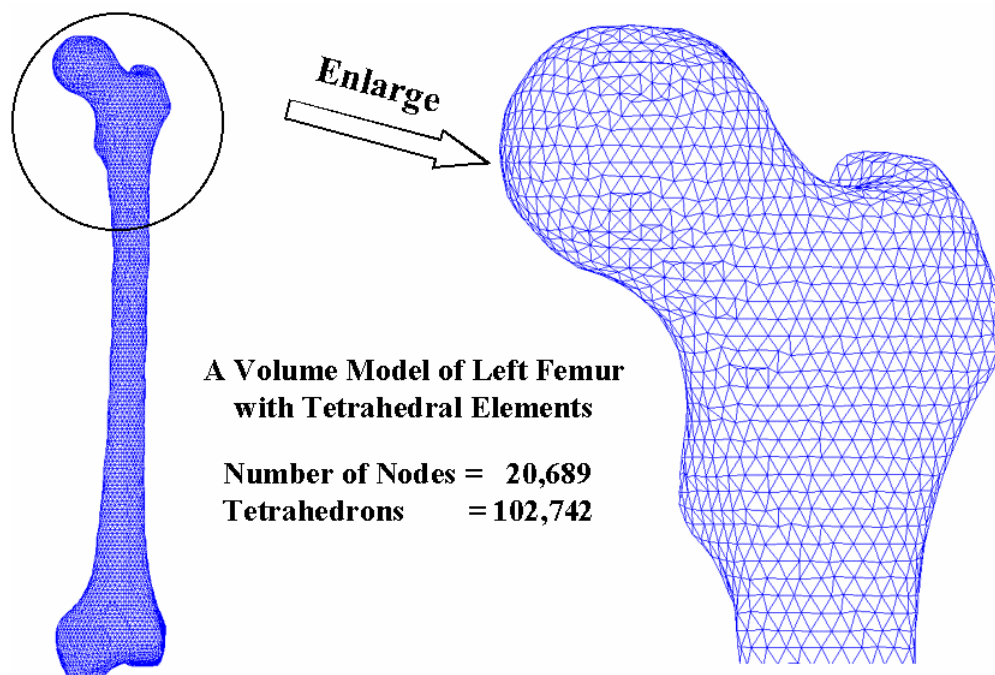


Figure 10. Volume Mesh of Femur

## MESH GENERATION FOR THE KIDNEY REGION:

The kidney region contained many major organs, such as kidneys, liver, duodenum, spleen, ascending colon, descending colon, transverse colon, and small intestine. The arbitrary shape of the tissue surfaces is obvious in the surface meshes created from the Visible Male, [Figure 11](#). A volume mesh containing 193,624 nodes and 895,475 tetrahedral volume elements was created



automatically with the volume mesh generator and is displayed in [Figure 12](#). The figure demonstrates that multiple material boundaries were preserved with fidelity.

Though the volume mesh of all the tissues was created simultaneously, we can zoom in and isolate the left kidney or descending colon as in [Figure 13](#) and [Figure 14](#), respectively. The volume meshes have a more gradual blending of different sized, regular-shaped triangle surfaces. It is a direct consequence of the deltahedral building block used.

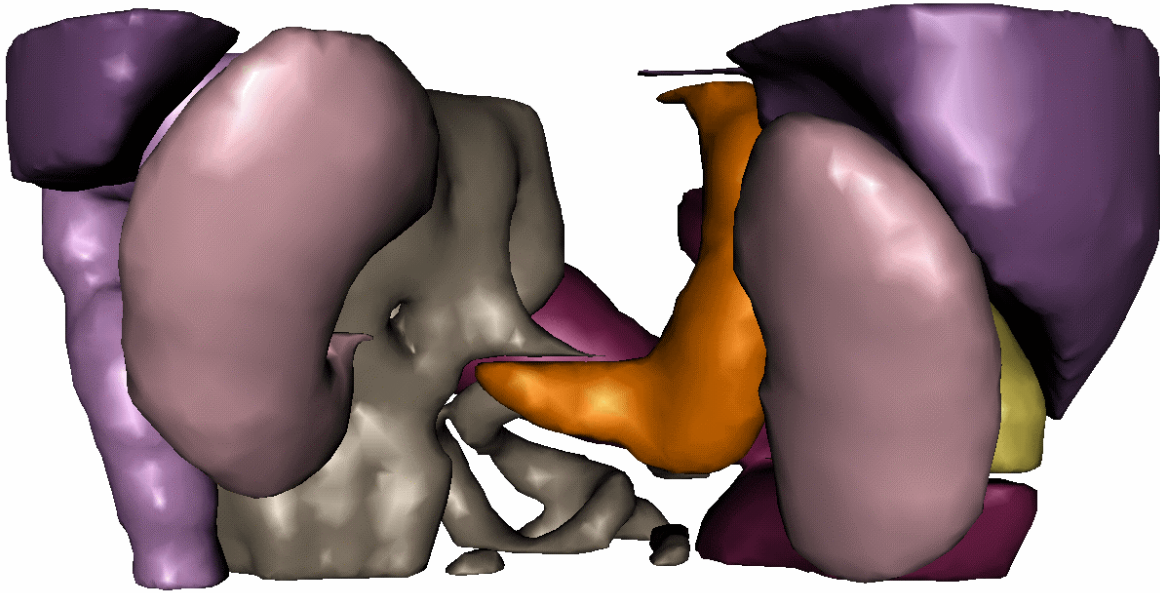


Figure 11. Surface Mesh of Tissues at Kidney Area

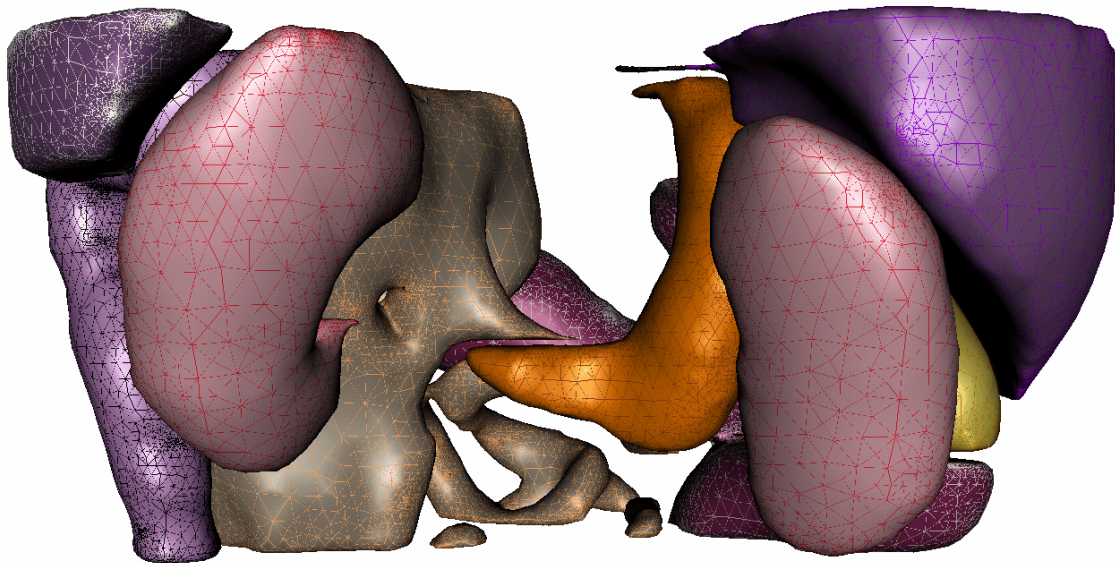
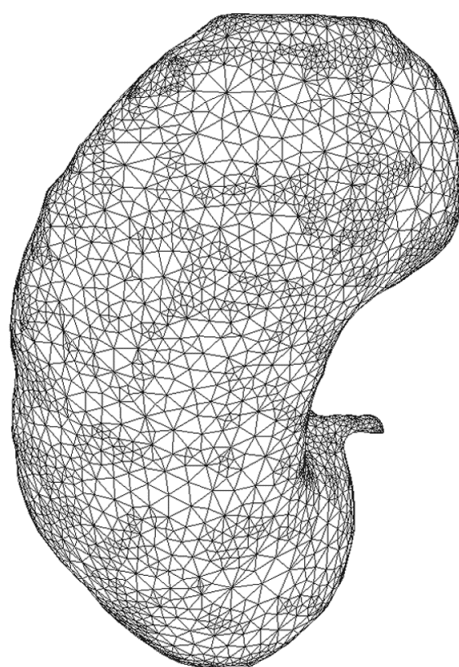
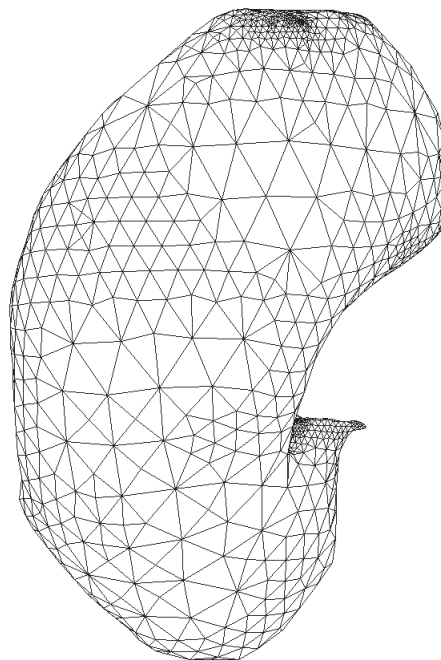


Figure 12. Volume Mesh of Tissues at Kidney Area

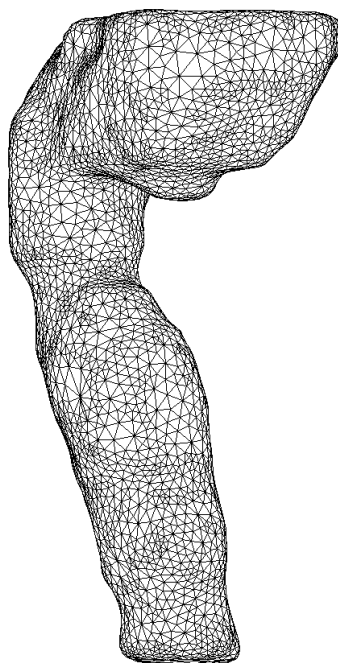


**Surface Mesh**

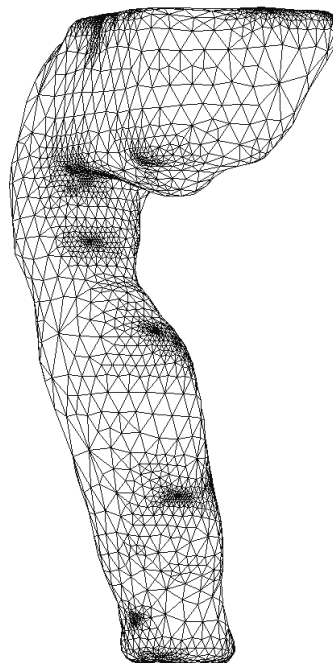


**Volume Mesh**

Figure 13. Surface and Volume Meshes of Left Kidney



**Surface Mesh**



**Volume Mesh**

Figure 14. Surface and Volume Meshes of Descending Colon

## **CONCLUSION:**

A mesh generation system was developed, which can generate high quality three-dimensional tetrahedral meshes from a set of medical images. This system involves image segmentation, surface mesh generation, adjustment, and volume mesh generation sub-systems. Each sub-system was discussed and implemented.

The validity of this new mesh generation strategy and implementation was demonstrated via the numerous anatomically accurate finite element tetrahedral models presented. The volumetric finite element models were full three dimensional, conforming tetrahedral elements. Within each of the models presented the arbitrary nature of the physical boundaries was evident. Multiple material boundaries were preserved in each mesh with fidelity.

## **ACKNOWLEDGEMENT:**

This work was supported, in part, by NIH Grants: R01 CA37245-09 and P01 CA80139 with Dartmouth College as the lead institution.

## **REFERENCES:**

1. M. J. Ackerman, The Visible Human Project, Proceedings of the IEEE, March 1998, Vol. 86, No. 3, pp. 504-511.
2. W. E. Lorensen and H. E. Cline, "Marching Cube: A High Resolution 3D Surface Construction Algorithm", Computer Graphics, July 1987, V 21, No 4.
3. W. E. Lorensen, "Marching through the Visible Man", IEEE Visualization Conference, 1995, pp. 368-373.
4. P. Bourke, "Polygonising a Scalar Field", <http://www.swin.edu.au/astronomy/pbouke/modelling/polygonise/>.
5. Schroeder W., Martin K., Lorensen B., "The Visualization Toolkit, An Object-Oriented Approach to 3D Graphics", Prentice Hall, 1997.
6. J. M. Sullivan, Jr., G. Charron, and K. D. Paulsen, "A Three Dimensional Mesh Generator for Arbitrary, Multiple Material Domains", Journal of Finite Elements in Analysis and Design, 1997, V 25, No. 2, pp. 219-241.
7. K. D. Paulsen, X. Jia, and J.M. Sullivan, Jr., "Finite Element Computations of Specific Absorption Rates in Anatomically-Conforming Full-Body Models for Hyperthermia Treatment Analysis", IEEE Trans. on Biomed. Eng., 1993, V 40, No.9, pp 933-945.
8. Z. Wu, J. M. Sullivan, Jr., J. Q. Zhang, "Automatic Refinement within an Adaptive Mesh Generation System", 7<sup>th</sup> International Conference on Numerical Grid Generation in CFS, September 23-28, 2000, Whistler, British Columbia, Canada;